Journal of Applied Polymer Science

# Synthetic Ni-talc as filler for producing polyurethane nanocomposites

**Manoela Argenton Prado,[1] Guilherme Dias,[1] Carlos Carone,[1,2] Rosane Ligabue,[1,2] Angela Dumas,[3] Christophe Le Roux,[3] Pierre Micoud,[3] François Martin,[3] Sandra Einloft[1,2]**

[1]Programa de Pós-Graduação em Engenharia e Tecnologia de Materiais (PGETEMA)—Pontifícia Universidade Católica do Rio Grande do Sul (PUCRS), Porto Alegre, Brazil

[2]Faculdade de Química (FAQUI)—Pontifícia Universidade Católica do Rio Grande do Sul (PUCRS), Porto Alegre, Brazil

[3]ERT 1074 Géomatériaux—GET UMR 5563 CNRS—Université de Toulouse, Toulouse, France

Correspondence to: S. Einloft (E-mail: einloft@pucrs.br)

**ABSTRACT:** New synthetic Ni-talc was used as filler in the synthesis of polyurethane (PU) nanocomposites by *in situ* polymerization and to emphasize the contribution of the new material compared with natural talc. Good dispersion of Ni-talc was supported by homogeneous green coloration observed in the polymer matrix. X-ray diffraction (XRD) analyses indicate the intercalation of polymeric matrix into the filler layers by the increase in $d_{001}$-spacing value of the Ni-talc for the nanocomposites when compared to the pristine filler. The nanocomposites obtained with synthetic talc showed an improvement in the crystallization temperature and in thermal stability when compared to pure PU and the composite obtained with natural talc. The young modulus of PU/talc materials containing both Ni-talc and natural talc were slight higher than pure PU. As shown by scanning electron microscope (SEM), Ni-talc fillers were well dispersed into the polymeric matrix probably due to the good compatibility of both phases filler/polymer mainly achieved by the filler OH interaction with the urethane group of the polymeric chain. © 2014 Wiley Periodicals, Inc. J. Appl. Polym. Sci. **2015**, *132*, 41854.

**KEYWORDS:** composites; mechanical properties; nanoparticles; nanowires and nanocrystals

Received 14 July 2014; accepted 6 December 2014
**DOI: 10.1002/app.41854**

## INTRODUCTION

The use of inorganic fillers into polymeric matrix improves their thermal, mechanical, and physical properties and also is a way of reducing costs. These fillers are in general in microscale. When nanometric fillers are used to produce nanocomposites materials, the properties are maximized due to the increase in the contact surface between the filler and the polymeric matrix.[1,2] Carbonates, sulfates, aluminum silicates, metallic oxides, and talc are the most commonly used fillers.[3,4] The use of natural talc as a filler to polymeric matrix is an interesting option due to their low cost.[5,6] Despite their good performance as filler, natural talc presents some drawbacks. One of the main limitations is the particle size, and natural talc cannot be homogeneously grounded below 1 μm without becoming amorphous and having their structure destroyed.[6–8] The association of other minerals and the substitution for different elements into the structure of natural talc also appear as disadvantages. Elements such as iron, manganese, and nickel among others can be present into the natural talc structure by isomorphic substitution of $Mg^{2+}$ by $Fe^{2+}$, $Mn^{2+}$, $Ni^{2+}$, resulting in an inhomogeneous chemical structure.[6–10] The use of synthetic talc allows to obtain samples with a well-defined chemical composition and high purity, besides the possibility of the crystallinity control, the particle size, and the layer thickness.[6,7] The use of natural talc is well known in literature. This filler has been used in the production of composites with different polymeric matrix, such as poly(vinyl alcohol),[11] LLDPE/MWCNT,[5] thermoplastic polyurethane,[12] thermoplastic polyurethane/polypropylene blends,[13,14] poly(L-Lactide),[15] polypropylene,[16–19] poly(lactic acid),[20] among others. Yousfi *et al* described the use of new synthetic talc as nanofillers reinforcement for polypropylene and polyamide 6 systems[6] and polypropylene/polyamide 6 blends.[21]

As polymeric matrix, the polyurethanes (PU) must be highlighted. These polymeric materials can have their chemical, physical, and mechanical properties designed by different possible combination of polyols and diisocyanates. For this reason, PU can find different niches of applications, such as coatings, adhesives, foams, thermoplastic elastomers, among others. They possess good mechanical properties but present low thermal stability and barrier properties.[22]

The main goal of this study is to present the syntheses and characterizations of PU nanocomposites comparing new

synthetic Ni-talc with the natural talc. The new nanocomposites materials were obtained by *in situ* polymerization and characterized regarding the nanocomposites formation, morphology, thermal, and mechanical properties.

## EXPERIMENTAL

### Materials

The synthesis of PU matrix was performed from the reaction between poly (caprolactone) diol (PCL, $M_n = 2000$ g mol$^{-1}$, Sigma-Aldrich) and 1,6-diisocyanatohexane (HDI, for synthesis, Merck) using a molar ratio of NCO/OH of 1 : 1. Dibutyl tin dilaurate (DBTDL, Miracema-Nuodex Ind.) was used as catalyst (0.1% w/w) and methyl ethyl ketone (MEK, P.A., Merck) as solvent (about 50 mL). The natural talc was obtained from F. Martin collections (reference T111 talc from Trimouns Ore, France), and Ni-talc fillers were obtained according to literature procedures.[8,23]

### Nanocomposites Syntheses

The reactions were carried out in a glass reactor of 500 mL equipped with five inputs, in which a mechanical stirring, thermocouple for temperature control (40°C), reflux system, and an addition funnel were attached. The reactions were performed in one step and conducted under nitrogen atmosphere. The talc samples were dispersed in methyl ethyl ketone in ultrasound equipment for 60 min and added in the beginning of the polymerization reactions. The fillers were added in percentages by weight of 0.5, 1, 2, 3, and 5%, taking into account the mass of polymer formed during the homopolymerization reaction.

### Characterization Methods

The progress of the reactions were followed by Fourier transform infrared spectroscopy (FTIR—Perkin Elmer FTIR spectrometer model Spectrum100) as well as the incorporation of Ni-talc, which was confirmed by the changes in the area of the characteristics bands in relation to pure PU. The XRD patterns were recorded on an INEL CPS 120 powder diffractometer with CoK$\alpha_{1+2}$ radiations between 0.334 and 127.206°2$\theta$ with a step size of 0.032 (GET, University of Toulouse).

The coherent scattering domain (CSD) size in the c* direction was calculated as described in the literature.[7] The nitrogen adsorption/desorption isotherms were determined at 77 K, using a volumetric method, with a Quantachrome Autosorb-1 apparatus (GET laboratory, University of Toulouse). The isotherms were recorded in the 0.05–0.3 relative pressure range, and high-purity nitrogen was used. Samples were outgassed for 15 h at 120°C under vacuum before analysis. Surface areas were calculated using Brunauer–Emmett–Teller (BET) method.[24]

The number average molecular weight ($M_n$), weight average molecular weight ($M_w$), and molecular weight distribution were obtained by gel permeation chromatography (GPC) using a liquid chromatograph equipped with an isocratic pump-1515 (eluant: tetrahydrofuran (THF), flow: 1 mL min$^{-1}$) and refractive index detector −2414 Waters Instruments with styragel column set.

Differential scanning calorimetry (DSC) (TA Instruments model Q20 equipment) was used to measure the material's melting temperature ($T_m$) and crystallization temperature ($T_c$). The DSC analyses were performed in two heating cycles, and the second was used to collect the data. The thermogravimetric analyses were performed in a SDT equipment (TA Instruments model Q600). The tests were carried out in a temperature range from 25°C to 900°C with a heating rate of 20°C min$^{-1}$. The TGA and DSC results were performed in duplicate, and the results were repeatable.

The samples were also analyzed by dynamic mechanical thermal analysis (DMTA) (TA Instruments Model Q800 equipment) for thermomechanical tests. Stress/strain tests were carried out, at 25°C, with rectangular shape films measuring thickness close to 0.15 mm, length 12 mm, and a width of approximately 7.0 mm. The Young moduli of the materials were determined according to ASTM D638. The analyses were carried out in triplicate.

For the assessment of distribution of the fillers in the polymer matrix, the scanning electron microscopy (SEM) mode secondary electrons (SE) aided by X-ray spectrometer for scattered energy was used.

## RESULTS AND DISCUSSION

### FTIR Analysis

In order to compare the behavior of the nanocomposites obtained with the new synthetic Ni-talc, we also performed reactions aiming to obtain composite material with natural talc (3 wt % natural talc) as filler. Figure 1(A) presents the FTIR spectra of these materials. The region around 3700 cm$^{-1}$ is characteristic of metal-OH bond, in the case of Ni-talc is attributed to $Ni_3$-OH and for natural talc is attributed to $Mg_3$-OH.[25,26] The band at 1040 cm$^{-1}$ and 670 cm$^{-1}$ are characteristic of the Si—O bond. In the regions of 1014 cm$^{-1}$ and 460 cm$^{-1}$ bands corresponding to the bond Si—O—Si, while the bond Ni—OH appears at 550 cm$^{-1}$ and 438 cm$^{-1}$ and the region of 709 cm$^{-1}$ and 669 cm$^{-1}$ corresponds to the free OH of the talc structure.[10–28]

The synthetic Ni-talc, the pure PU, and the nanocomposites PU Ni-talc were also characterized by infrared spectroscopy, and the assignment of the bands performed in agreement with those described in literature.[10,25,26,28] Figure 1(A) presents the IR spectra of Ni-talc, pure PU, and as an example the nanocomposite PU Ni-talc 3 wt % and the composite PU 3 wt % natural talc. For pure PU and the composites, the bands in 3444 and 3385 cm$^{-1}$ can be attributed to the N—H of the urethane bond. The bands in the region of 2939 and 2864 cm$^{-1}$ can be assigned to different vibrational modes of the $CH_2$ group. The band at 1727 cm$^{-1}$ is characteristic of the C=O group of the urethane bond. The region of 1528 cm$^{-1}$ shows characteristic bands for CN and NH bonds of the urethane groups. The CO—O group bond appears at 1235 cm$^{-1}$. In the regions of 1096, 1065, and 1042 cm$^{-1}$, the bands relatives of N—CO—O and C—O—C groups are observed.[29] A band at 1159 cm$^{-1}$ can be assigned to the C—O—C group of the soft segment of the polymeric chain.

The incorporation of the Ni-talc into the PU matrix can be confirmed by the intensity of the characteristic bands of the filler, which increases, with the augmentation of the filler content in the composites until 3%. The nanocomposite PU Ni-talc 5 wt % presented a decrease in the band when compared to the nanocomposite PU 3 wt % Ni-talc probably by the filler

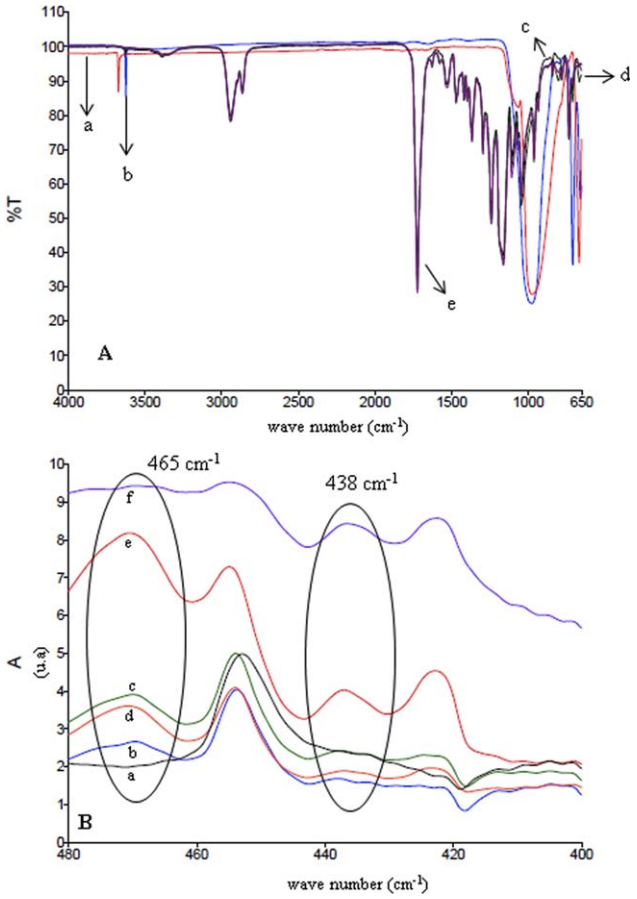


**Figure 1.** (A) FTIR spectra of natural talc (a), Ni-talc (b), pure PU (c), PU 3 wt % Ni-talc (d), PU 3 wt % natural talc (e) (B) pure PU (a), PU 0.5 wt % Ni-talc (b), PU 1 wt % Ni-talc (c), PU 2% Ni-talc (d), PU 3% Ni-talc (e), PU 5% Ni-talc (f). [Color figure can be viewed in the online issue, which is available at wileyonlinelibrary.com.]

agglomeration, which results in a poor filler distribution, as shown in Figure 1(B). This behavior can be highlighted in the region of 465 $cm^{-1}$ characteristic of the oxygen of the talc structure and in the region of 438 $cm^{-1}$ characteristic of the Ni—OH.[10]

### Structural Analysis by DRX

Aiming to evaluate the crystalline structure of Ni-talc and compare with natural talc, the X-ray diffraction analysis was performed in both samples and is shown in Figure 2.

Synthetic talc presents the most characteristic peaks of the natural talc as presented by Dumas *et al.*[8] When compared to natural talc, the synthetic has less intense and broader peaks. The coherent scattering domain (CSD) size in the c* direction gives an estimation of the stacking order of the layers.[7] The calculated value for synthetic talc was 31 nm and for natural talc 85.2 nm. The CSD size from synthetic talc is less than half of the size of natural talc indicating the better crystallinity of the latter.

Figure 2 also presents the X-ray diffraction patterns for the nanocomposites obtained with different filler contents. For pure Ni-talc and for the nanocomposites, a broad diffraction halo is seen near $d = 9.5$ Å which is associated with Ni-talc. For the nanocomposites, we can observe an increase almost linear in this peak with the increase in the filler content. The nanocomposite PU 5 wt % Ni-talc does not present the same behavior probably by the filler agglomeration resulting in an inhomogeneous filler distribution.

Figure 2 evidences an increase in Ni-talc in polymer matrix, and the interaction of the filler galleries with the polymeric matrix. These observations can be corroborated by the comparison of the CSD value of Ni-talc (31 nm) and in the nanocomposites presented in Figure 3, as well as the interlayer spacing of the Ni-talc ($d = 0.9$ *nm*) and of the nanocomposites. For example, $d_{001}$-spacing of the filler in the nanocomposite 0.5 wt % Ni-talc increased from 0.9 nm for the pristine Ni-talc to 1.1 nm in the nanocomposite evidencing an intercalation and not a exfoliation of the filler into the polymeric matrix.[30] With the increasing of the filler, the $d_{001}$-spacing value remained constant $d_{001} = 1.1 nm$, but the CSD value decreased from 108 nm for the nanocomposite with 0.5 wt % of filler to 78 nm to the

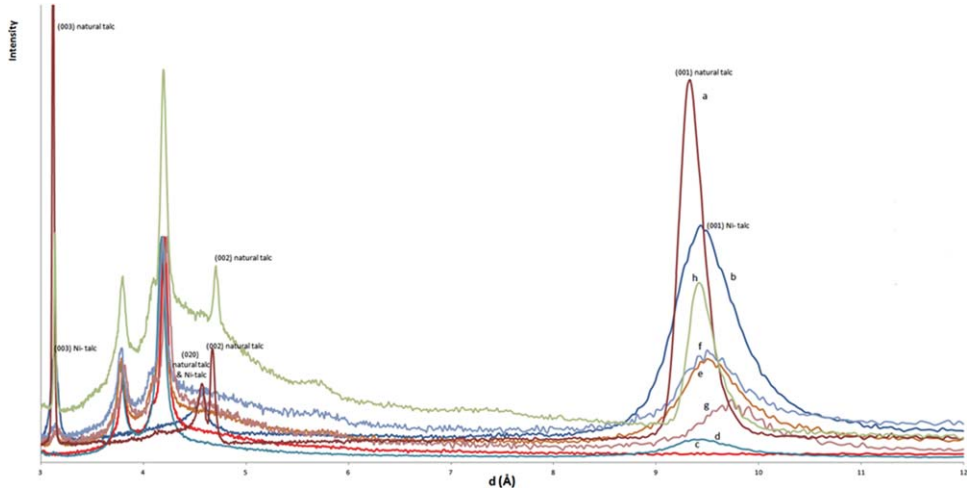


**Figure 2.** X-ray diffraction patterns of Ni-talc (a) and natural talc (b), pure PU (c), PU 1 wt % Ni-talc (d), PU 2 wt % Ni-talc (e), PU 3% Ni-talc (f), PU 5% Ni-talc (g), PU 3 wt % natural talc (h). [Color figure can be viewed in the online issue, which is available at wileyonlinelibrary.com.]

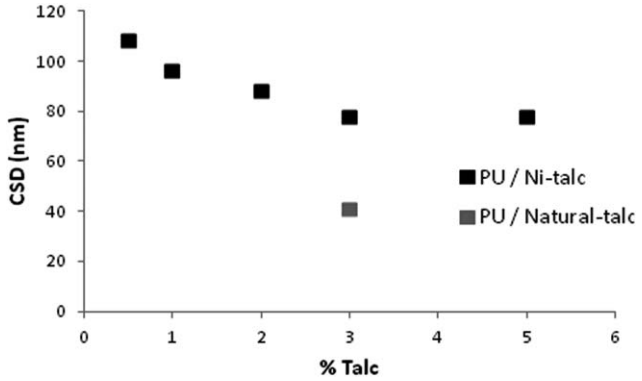


**Figure 3.** CSD calculated to Ni-talc and natural talc nanocomposites.

nanocomposite with 3 and 5 wt % of filler indicating a tendency to a better filler distribution until 3 wt %. The sample with 5 wt % presented a sharp peak indicating that some part of the filler agglomerate.[30] The natural talc presented a decrease in the coherence value decreasing from 81.2 nm in pristine natural talc to 41.2 nm in the composite PU natural talc 3 wt % indicating the good incorporation of the filler into polymeric matrix.

The Ni-talc presents a green color allowing to see visually the incorporation of this filler by the color change of the obtained materials. Figure 4 presents the films of the PU/Ni-talc nanocomposites with different filler content.

### Molar Mass Analysis

The obtained nanocomposites were characterized by GPC analysis, and the molar mass decreased with the increase in the filler content. The pure PU presents a $M_n$ of 49,300 g mol$^{-1}$ and $M_w$ of 73,673 g mol$^{-1}$. When 0.5 wt % of the filler was added a slight decrease in the molar mass was evidenced ($M_n = 44{,}206$ g mol$^{-1}$ and $M_w = 68{,}103$ g mol$^{-1}$). When the filler content reached 5 wt %, it was observed an important decrease in molar mass ($M_n = 14{,}666$ g mol$^{-1}$ and $M_w = 21{,}922$ g mol$^{-1}$). These results corroborate the influence of the OH during the polymerization reaction, which must compete with the OH of the poliol during the reaction as observed for nanocomposites PU/$TiO_2$.[3]

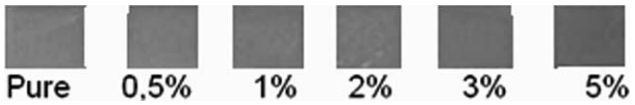


**Figure 4.** PU and nanocomposites films obtained with different filler content.

Natural talc presented a similar behavior as Ni-talc for 3% in weight of filler content ($M_n = 22{,}830$ g mol$^{-1}$; $M_w = 34{,}364$ g mol$^{-1}$ for Ni-talc; $M_n = 23{,}859$ g mol$^{-1}$; $M_w = 34{,}927$ g mol$^{-1}$ for natural talc).

### Thermal Stability

Figure 5 presents the DSC results for the Ni-talc nanocomposites in different concentrations of the filler as well as for natural talc (3 wt %).

From Figures 5 and 6, it can be highlighted an increase in crystallization temperature of the Ni-talc nanocomposites with the filler content. This behavior can be explained by the fact that the Ni-talc having an ordered structure with high specific surface area (BET value of 135 $m^2g^{-1}$) acts as a nucleating agent, thus facilitating crystallization.[12–14] Natural talc composites presented a $T_c$ similar to pure PU. Besides the high-ordered structure of the natural talc, its low specific surface area, (BET value of around 20 $m^2g^{-1}$),[6,8] when compared to synthetic Ni-talc must be the responsible by the suppression of the improvement of the crystallization temperature of the composites PU talc. The melting temperature values do not change as the $T_c$ values, but we can see a tendency to increase with the increasing in the filler content for the nanocomposites obtained by *in situ* polymerization using synthetic Ni-talc. Muller *et al*[5] found that the melting temperature did not change with the addition of 10–30 wt % of talc (Luzenac 7), and the crystallization temperature was slight affected for the composite LLDPE filled with MWCNTs and a content of 30 wt % of talc. They also found that for particles in microsize scale, the size of the particles did not show significant variations on the crystallization behavior.[5]

The onset temperatures of the nanocomposites are presented in Figure 7. For the samples obtained with Ni-talc, an increase in the $T_{onset}$ is evidenced for all cases when compared to pure PU.

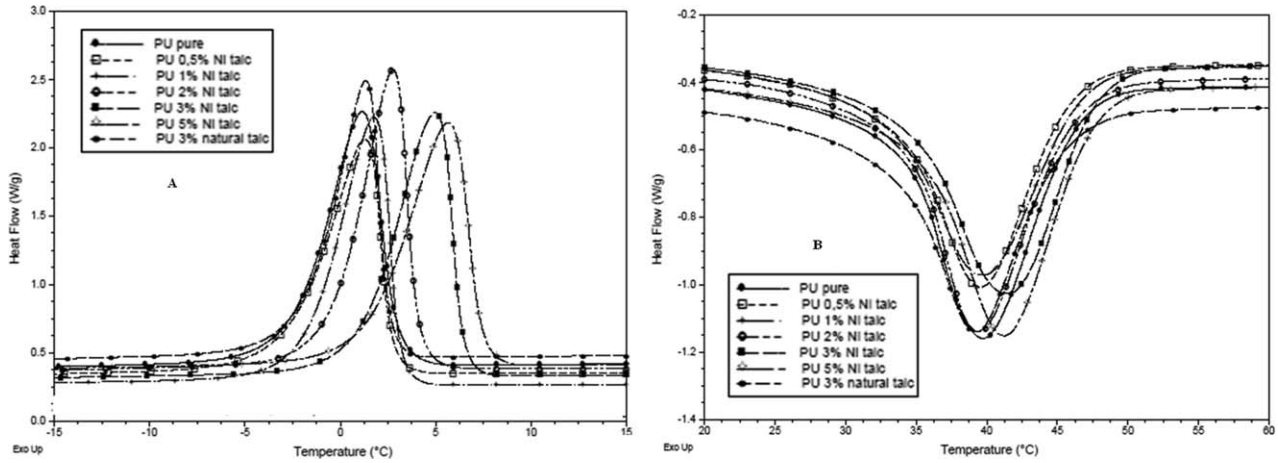


**Figure 5.** DSC analyses for pure PU and for nanocomposites obtained by *in situ* polymerization (A) crystallization curve (*Tc*) and (B) melting curves (*Tm*).

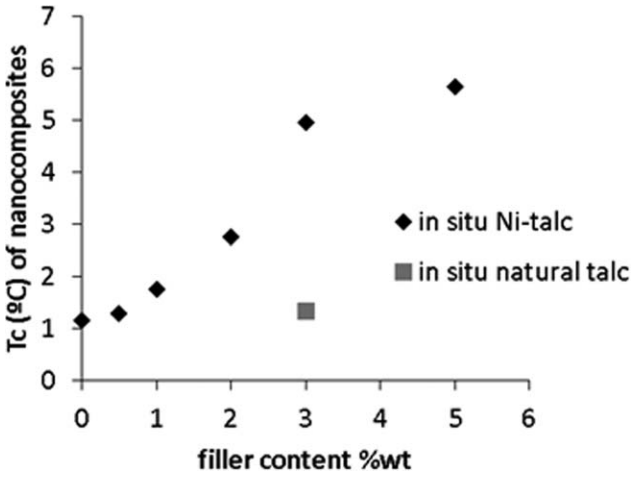


**Figure 6.** Crystallization temperatures for nanocomposites.

This behavior was also described in literature for thermoplastic polyurethane/polypropylene blends.[13] When natural talc was used as filler, the $T_{onset}$ remains close to that obtained for pure PU. The same result was observed, when talc was added to thermoplastic polyurethanes.[12] These results indicate that the interaction of Ni-talc by the OH with the urethane group is probably more intense in the nanocomposites with Ni-talc. The specific surface area of natural talc measured by BET presents a maximum value around 20 $m^2g^{-1}$.[6,8] BET values for synthetic Ni-talc are higher (135 $m^2g^{-1}$) facilitating the OH group interactions with the polymer chain and improving the thermal behavior of Ni-talc nanocomposites when compared to composites obtained with natural talc. Yousfi *et al*[21] observed the same behavior for PP/PA6 blends in which the adittion of synthetic talc had a positive effect on thermal stability unlike natural talc.

For the DTG curves presented in Figure 8, it can be seen that the Ni-talc nanocomposites obtained by *in situ* polymerization shows an increase in the second peak of decomposition with the increase in the filler content. As previously reported in the literature,[3,31] this occurs due to the formation of a network structure by the interaction of the OH of the filler with the urethane

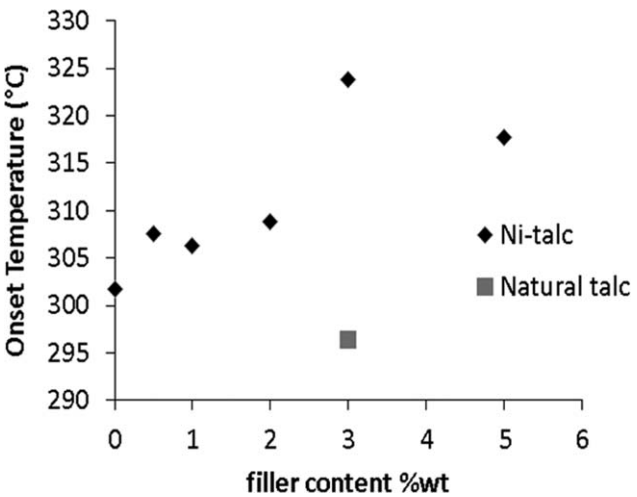


**Figure 7.** Tonset for the obtained nancomposites.

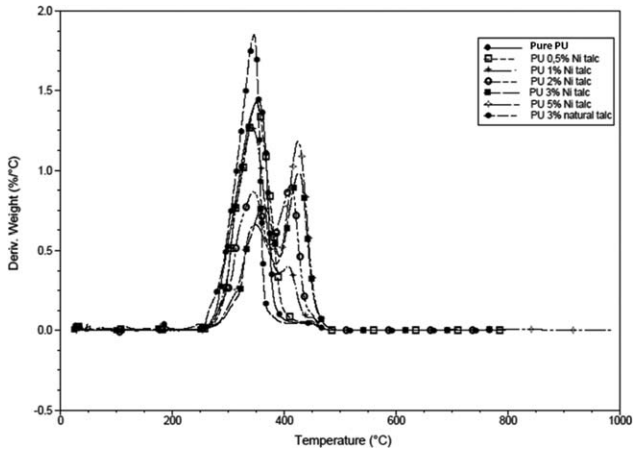


**Figure 8.** DTG curves for pure PU and for the nanocomposites.

group of the polymeric chain resulting in a barrier to volatile products formed during the decomposition process as well as a thermal insulator, increasing the degradation temperature of the nanocomposites until 3 wt % of filler. In the same Figure, we can also highlight the different behavior of all Ni-talc nanocomposites presenting two degradation events while natural talc presents one degradation peak. This behavior corroborates the advantages of synthetic Ni-talc presenting a higher specific surface area than natural talc imputing a synergetic effect of the filler with the polymeric matrix improving thermal properties of the nanocomposites. For example, the $T_{onset}$ for pure PU is 301.7°C and for a nanocomposite PU 3% Ni-talc is 323.8°C (+22.1°C). An important shift was also observed for $T_{max}$ of degradation. $T_{max}$ for pure PU is 374°C and for the 3 wt % Ni-talc nanocomposite is 445°C (+71°C compared to pure PU). The $T_{onset}$ decreased for the nanocomposite PU 5 wt % Ni-talc when compared to nanocomposite PU 3 wt % Ni-talc probably because of the interaction filler/filler became more important than the interaction filler/polymer.

### Mechanical Properties

The results of stress/strain are shown in Figure 9 and Table I. The Ni-talc nanocomposites (0.5 wt %, 1 wt %, and 2 wt %)

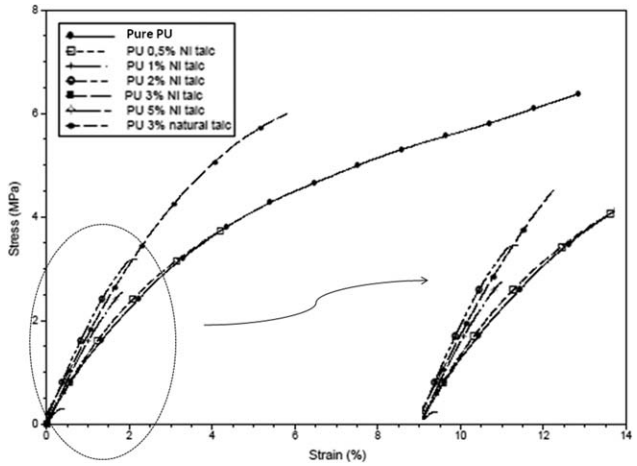


**Figure 9.** Stress/strain (by DMA) of nanocomposites synthesized with 0, 0.5, 1, 2, 3, and 5 wt % of Ni-talc and 3 wt % of natural talc.

**Table I.** Mechanical Properties of the Nanocomposites PU Ni-talc and PU Natural Talc

| Sample | Stress at break (Mpa) | Strain at break (%) | Young modulus (Mpa) |
|---|---|---|---|
| Pure PU | 6.1 ± 0.4 | 9.7 ± 0.6 | 1.5 ± 0.1 |
| PU 0.5% Ni-talc | 4.2 ± 0.9 | 4.9 ± 0.7 | 1.6 ± 0.2 |
| PU 1% Ni-talc | 2.4 ± 0.3 | 1.6 ± 0.4 | 1.7 ± 0.2 |
| PU 2% Ni-talc | 3.4 ± 0.3 | 2.23 ± 0.05 | 1.6 ± 0.2 |
| PU 3% Ni-talc | 0.6 ± 0.3 | 0.6 ± 0.1 | 1.47 ± 0.09 |
| PU 5% Ni-talc | 0.6 ± 0.2 | 0.6 ± 0.2 | 1.64 ± 0.02 |
| PU 3% Natural talc | 5.8 ± 0.2 | 6.2 ± 0.4 | 1.43 ± 0.01 |

presented higher values of stress in lower deformations when compared to pure PU. The materials with 3 wt % and 5 wt % of filler are fragile and presented low stress values. The decrease in stress values at higher filler load is probably due to the replacement of filler matrix continuity by filler–filler contact,[17] or by the increase in the cross-link formed between the polyurethane and the talc. When compared to 3 wt % Ni-talc nanocomposite, the composite obtained with natural talc in the same composition presented a superior stress values in higher deformation values. These results corroborate that parameters such as filler interfacial adhesion, concentration, dispersion, and distribution affects the mechanical properties of the composites.[18]

Young moduli of both PU/talc composites containing Ni-talc or natural talc were slight higher than pure PU. The maximum increment was achieved to the sample of 1 wt % Ni-talc, which presented an increase of 5.7% when compared to pure PU.

### SEM Analysis

Figure 10 shows the SEM images of Ni-talc nanocomposites with different filler content as well as PU/natural talc composite with 3 wt %. It could be highlighted that both are well dispersed in polyurethane matrix suggesting a good compatibility of talc with the polymeric matrix. The talc fillers can interact with the hard segments of the polyurethane through the Ni-OH and Si-OH groups on the edges of the talc layers allowing a good dispersion of the filler without the addition of coupling agents. The same behavior was related for PVA/talc and PVA/$CaCO_3$ composites evidencing the important role of the OH present in both talc and $CaCO_3$ allowing a good dispersion of the fillers.[30] In SEM images of nanocomposites, Ni-talc with 3 and 5 wt % of filler can be observed a more important change in the morphology with the nucleation points more evidenced. The crystallization temperature ($T_c$) of both was higher when compared to pure PU and the nanocomposites with 0.5 wt %, 1 wt %, and 2 wt % (Figure 6). These changes allied to a good dispersion of the filler affect directly the thermal and mechanical properties.[20,32,33]

When the SEM image of the nanocomposite PU 3 wt % Ni-talc is compared to the composite of natural talc with the same filler content, it can realize the difference in the polymer morphology. The polymer grains are larger in the composites obtained with natural talc when compared to Ni-talc and an agglomeration of the filler can be noticed in the grain boundary. This can give an indication of the different thermal properties obtained for the two materials.

The cryofractured images presented in Figure 11 evidences that the pure PU presents a crack growth randomly distributed on the surface. The nanocomposites PU Ni-talc presents a different

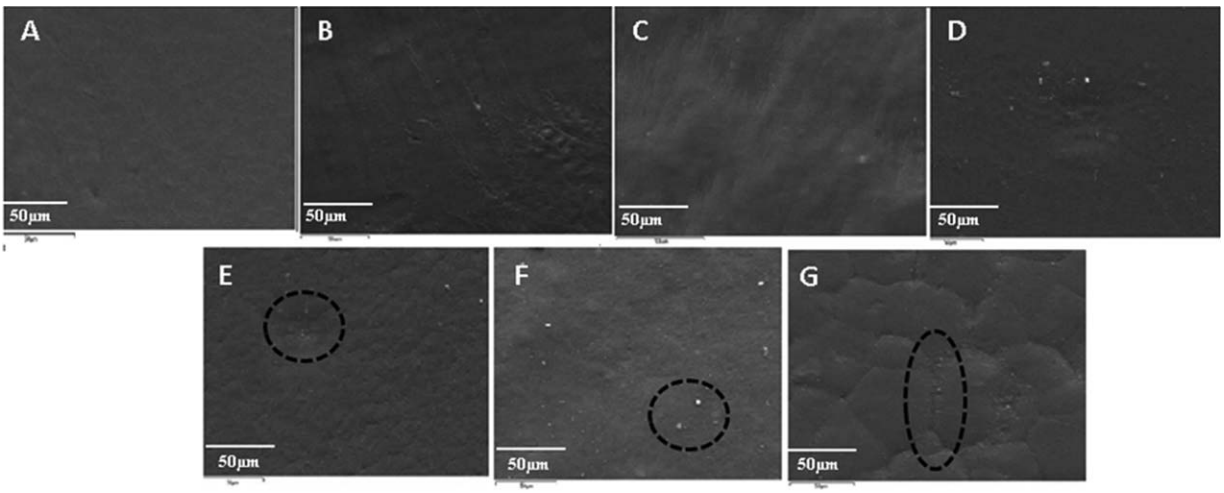


**Figure 10.** SEM micrographs of the materials at magnification of 10,000x; pure PU (A), nanocomposites PU 0.5 wt % Ni-talc (B), PU 1% Ni-talc (C), PU 2% Ni-talc (D), PU 3% Ni-talc (E), PU 5% Ni-talc (F), and (G) PU 3% natural talc.

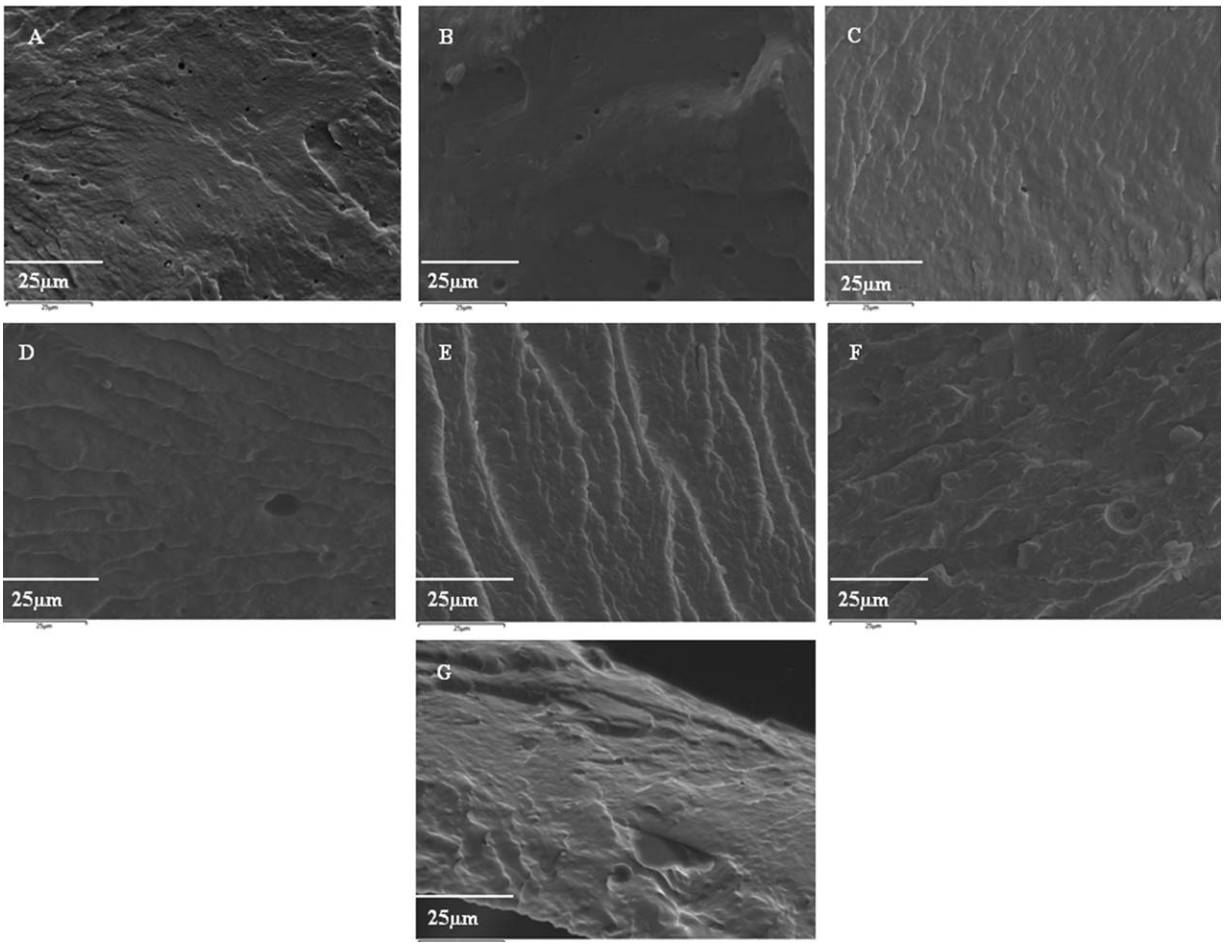


**Figure 11.** SEM micrographs from fractures, mode SE, of materials at magnification of 2,000x; pure PU (A), nanocomposites PU 0.5 wt % Ni-talc (B), PU 1% Ni-talc (C), PU 2% Ni-talc (D), PU 3% Ni-talc (E), PU 5% Ni-talc (F), and PU 3% natural talc (G).

morphology with a rough ordered fractured surface indicating the good dispersion and interfacial adhesion of filler and polymeric matrix. The nanocomposite PU 5 wt % Ni-talc presents agglomeration points that can be considered as weak points reducing the properties due to the stress concentration. The SEM surface analyses and the fracture analyses of the pure PU, the nanocomposites PU Ni-talc, and the composite PU natural talc showed that different morphologies result in different thermal and mechanical behavior as well as the agglomeration points degrades both the thermal and mechanical properties as evidenced for sample PU 5 wt % Ni-talc.

## CONCLUSIONS

A series of nanocomposites of polyurethane were prepared by *in situ* polymerization using new synthetic Ni-talc as filler and compared to natural talc. The content of Ni-talc can influence the thermal and mechanical properties as well as the morphology of the nanocomposites. The best thermal properties were achieved when 3% of Ni-talc was used, and the results were superior when compared to natural talc. The XRD analysis has indicated the dispersion in the matrix and intercalation of the polymeric matrix into the filler layers by the increase in $d_{001}$-spacing value of the Ni-talc for the nanocomposites when compared to the pristine filler. The new synthetic Ni-talc particles improved the thermal properties and increased the crystallization temperature unlike natural talc.

## ACKNOWLEDGMENTS

The authors would like to thank PRONEX/FAPERGS for financial support. SE and RL acknowledge CNPq for DT grant and CC CAPES for PNPD post-doc fellowship.

## REFERENCES

1. Carrado, K. A.; Xu, L. *Chem. Mater.* **1998**, *10*, 1440.
2. Esteves, A. C. C.; Timmons, A. B.; Trindade, T. *Quim. Nova.* **2004**, *27*, 798.
3. Da Silva, V.; Santos, L. M.; Subda, S. M.; Ligabue, R.; Seferin, M.; Carone, C.; Einloft, S. *Polym. Bull.* **2013**, *70*, 1819.
4. Zia, K. M.; Bhatti, H. N.; Bhatti, I. A. *Reac. Funct. Polym.* **2007**, *67*, 675.
5. Muller, M. T.; Dreibe, J.; Haubler, L.; Krause, B.; Potschke, P. *J. Polym. Sci. Pol. Phys.* **2013**, *51*, 680.

6. Yousfi, M.; Livia, S.; Dumas, A.; Le Roux, C.; Crépin-Leblond, J.; Greenhill-Hooper, M.; Duchet-Rumeau, J. *J. Colloid Interface Sci.* **2013**, *403*, 29.
7. Dumas, A.; Martin, F.; Ferrage, E.; Micoud, P.; Le Roux, C.; Petit, S. *Appl. Clay Sci.* **2013**, *85*, 8.
8. Dumas, A.; Martin, F.; Le Roux, C.; Micoud, P.; Petit, S.; Ferrage, E.; Brendlé, J.; Grauby, O.; Greenhill-Hooper, M. *Phys. Chem. Miner.* **2013**, *40*, 361.
9. Chabrol, K.; Gressier, M.; Pebere, N.; Menu, M. J.; Martin, F.; Bonino, J. P.; Marichal, C.; Brendle, J. *J. Mater. Chem.* **2010**, *20*, 9695.
10. Martin, F.; Micoud, P.; Delmotte, L.; Marichal, C.; Le Dred, R.; De Parseval, P.; Mari, A.; Fortuné, J. P.; Salvi, S.; Béziat, D.; Grauby, O.; Ferret, J. *Can. Mineral.* **1999**, *37*, 997.
11. Wang, B.; Wang, Q.; Li, L. *J. Appl. Polym. Sci.* **2013**, *130*, 3050.
12. Amico, S. C.; Freitag, C. P. M.; Riegel, I. C.; Pezzin, S. H. *Revista Matéria.* **2011**, *16*, 597.
13. Bajsic, E. G.; Rek, V.; Pavic, B. O. *J. Elastom. Plast.* **2012**, *45*, 501.
14. Bajsic, E. G.; Rek, V.; Pavic, B. O. *J. Polym.* **2014**, *2014*, 1.
15. Jo, M. Y.; Ryu, Y. J.; Ko, J. H.; Yoon, J. S. *J. Appl. Polym. Sci.* **2013**, *129*, 1019.
16. Wang, K.; Bahlouli, N.; Addiego, F.; Ahzi, S.; Rémond, Y.; Ruch, D.; Muller, R. *Polym. Degrad. Stab.* **2013**, *98*, 1275.
17. Leong, Y. W.; Bakar, M. B. A.; Ishak, Z. A. M.; Ariffin, A.; Puzansky, B. *J. Appl. Polym. Sci.* **2004**, *91*, 3315.
18. Castillo, L. A.; Barbosa, S. E.; Capiati, N. J. *J. Polym. Res.* **2013**, *20*, 152.
19. Bakar, M. B.; Leong, Y. W.; Ariffin, A.; Ishak, Z. A. W. *J. Appl. Polym. Sci.* **2007**, *104*, 434.
20. Jain, S.; Misra, M.; Mohanty, A. K.; Ghosh, A. K. *J. Polym. Environ.* **2012**, *20*, 1027.
21. Yousfi, M.; Livi, S.; Dumas, A.; Crépin-Leblond, J.; Greenhill-Hooper, M.; Duchet-Rumeau, J. *J. Appl. Polym. Sci.* **2014**, *131*, 40453.
22. Salahuddin, N.; Abo-El-Enein, S. A.; Selim, A.; El-Dien, S. *Appl. Clay. Sci.* **2010**, *47*, 242.
23. Dumas, A.; Le Roux, C.; Martin, F.; Micoud, P. *Int Pat WO.* **2013**, *004*, 979.
24. Brunauer, S.; Emmett, P. H.; Teller, E. *J. Am. Chem. Soc.* **1938**, *60*, 309.
25. Zhang, M.; Hui, Q.; Lou, X. J.; Redfern, S. A. T.; Salje, E. K. H.; Tarantino, S. *Am. Mineral.* **2006**, *91*, 816.
26. Silva, C.; Fonseca, M.; Barone, J.; Airoldi, C. *Mater. Chem.* **2002**, *14*, 175.
27. Russell, J. D.; Farmer, V. C.; Velde, B. *Mineral. Mag.* **1970**, *37*, 870.
28. Fonseca, M. G.; Silva, C. R.; Barone, J. S.; Airoldi, C. *Mater. Chem.* **2000**, *10*, 789.
29. Chattopadhyay, D. K.; Raju, K. V. S. N. *Prog. Polym. Sci.* **2007**, *32*, 352.
30. Latinwo, G. K.; Aribike, D. S.; Susu, A. A.; Kareem, S. A. *Nat. Sci.* **2010**, *8*, 23.
31. Mishra, A. K.; Mishra, R. S.; Narayan, R.; Raju, K. V. S. N. *Prog. Org. Coat.* **2010**, *67*, 405.
32. Castillo, L.; López, O.; Zaritzky, N.; García, M. A. *Carbohydr. Polym.* **2013**, *95*, 664.
33. Castillo, L. A.; Barbosa, S. E.; Capiati, N. J. *J. Appl. Polym. Sci.* **2012**, *126*, 1763.